International Journal of Refrigeration 88 (2018) 248–259

Contents lists available at ScienceDirect

International Journal of Refrigeration

journal homepage: www.elsevier.com/locate/ijrefrig

Numerical modeling of a two-phase twin-screw expander for Trilateral Flash Cycle applications

Giuseppe Bianchi[a,*], Stuart Kennedy[b], Obadah Zaher[c], Savvas A. Tassou[a], Jeremy Miller[c], Hussam Jouhara[a]

[a] Brunel University London, Institute of Energy Futures, Centre for Sustainable Energy Use in Food Chains, Middlesex, Uxbridge UB8 3PH, United Kingdom
[b] Howden Compressors Ltd., Renfrew PA4 8XJ, United Kingdom
[c] Spirax Sarco Engineering PLC., Cheltenham GL51 9NQ, United Kingdom

ARTICLE INFO

Article history:
Received 8 November 2017
Revised 22 December 2017
Accepted 5 February 2018
Available online 21 February 2018

Keywords:
Trilateral Flash Cycle
Twin-screw expander
Two-phase expander
Low grade heat to power conversion
GT-SUITE™

ABSTRACT

This paper presents numerical investigations of a twin-screw expander for low grade (≤100 °C) heat to power conversion applications based on the bottoming Trilateral Flash Cycle. After a thorough description of the modeling procedure, a first set of simulations shows the effect of different inlet qualities of the R245fa working fluid and of the revolution speed on the expander performance. In particular, at 3750 RPM and an inlet absolute pressure of 5 bar, the volumetric and adiabatic efficiencies would increase from 24.8% and 37.6% to 61.2% and 83.1% if the inlet quality in the intake duct of the expander increased from 0 to 0.1. To further assess the effects of inlet quality, inlet pressure and revolution speed on the expander performance, parametric analyses are carried out in the ranges 0–1 inlet quality, 5–10 bar pressure and 1500–6000 RPM speed respectively.

Modélisation numérique d'un détendeur diphasique à deux vis pour les applications de cycle trilatéral-flash

Mots-clés: Cycle trilatéral-flash; Détendeur à deux vis; Détendeur diphasique; Conversion de chaleur à basse température en énergie; GT-SUITETM

1. Introduction

Energy demand and prices are continuing to rise in the global market and there is increasing scrutiny of industrial environmental impact. Nonetheless, recent estimations from Forman et al. (2016) state that the theoretical waste heat potential in industry, i.e. the share of primary energy consumptions that is not exploited for energy services (e.g. motion, heat, cooling, light and sound) and that can be effectively recovered (no losses by radiation, electrical transmission, friction etc.), can reach 918 TWh on a European scale and 62.2 PWh worldwide. The biggest share of this potential, 51% for the European one and 63% for the global one, occurs at temperatures below 100 °C. Examples of low temperature heat sources can be found in manufacturing processes, gas turbine generators as well as nuclear reactors and occur in the form of exhausts and effluents (McKenna and Norman, 2010). Although the iron and steel sector accounts for a large share of the low temperature waste heat potential, the growing interest in heat recovery technologies is broader. Extensive applied research has been indeed carried out in ceramics (Peris et al., 2015), paper and pulp (Öhman, 2012), metallurgical (Walsh and Thornley, 2012), oceanic (Tchanche et al., 2011), and solar thermal (Wang et al., 2013) sectors. A recovery of this energy and a further conversion into electricity would contribute to reduction of the environmental impact of the industrial process and, at the same time, would play a key role in decreasing overall plant operating costs.

Trilateral Flash Cycle (TFC) systems hold a good promise as an alternative to Organic Rankine Cycle (ORC) ones, concerning the exploitation of low temperature heat sources. In particular, although TFC systems consist of the same components as ORCs,

* Corresponding author.
E-mail address: giuseppe.bianchi@brunel.ac.uk (G. Bianchi).

https://doi.org/10.1016/j.ijrefrig.2018.02.001

Nomenclature

dx	discretization length [m]
e	specific total internal energy [J kg^{-1}]
h	specific enthalpy [J kg^{-1}]
m	mass [kg]
$\dot{m}$	mass flow rate [kg s^{-1}]
p	pressure [Pa]
r	specific internal energy [J kg^{-1}]
u	velocity at the boundary [m s^{-1}]
t	time [s]
x	quality
A	area [m^2]
B	total number of boundaries
C_f	Fanning friction factor
D	(equivalent) diameter [m]
H	heat transfer coefficient [W m^{-2} K^{-1}]
K_p	pressure loss coefficient
P_{ind}	indicated power [W]
R	equivalent gas constant [J kg^{-1} K^{-1}]
SF	scaling factor
T	temperature [K]
V	volume [m^3]
Z	number of cells
α	crank angle [°]
γ	ratio of specific heats
ζ	spatial reference [m]
η_{ad-is}	adiabatic-isentropic efficiency
η_{vol}	volumetric efficiency
μ	dynamic viscosity [Pa s]
ρ	density [kg m^{-3}]
ω	revolution speed [RPM]
$\Delta\alpha$	angular cycle duration [°]
$_{01}$	total upstream conditions
$_{2}$	static downstream conditions
$_{is}$	isentropic
$_{leak}$	leakage
$_{s}$	heat transfer surface
$_{suc}$	suction

there is a major difference related to the state before the expansion process. In fact, the working fluid in a TFC does not evaporate but instead it expands from the saturated liquid state and according to a flashing evaporation phenomenon that gives the name to the thermodynamic cycle. The 3-leg cycle configuration allows a closer matching between the temperature profiles of heat source and the working fluid since the heat gain does not lead to any phase change in it.

Availability of research works on TFC systems is limited. A reference work in this topic is Smith (1993), where the author performed a comparison between the subcritical and supercritical ORCs and a TFC, aiming at maximizing the net power output for any given heat source temperature between 100 and 200 °C. The author concluded that TFC had superior performance within all the temperature ranges and for any fluid combination. Furthermore, he argued that the gross electrical output of TFC varied insignificantly with the choice of the working fluid, due to the effective heat transfer between streams in liquid phase. Moreover, Fischer (2011) compared a TFC using water and four ORC configurations. An isentropic efficiency of 0.85 for the expanders of both cycles was assumed. The findings revealed 14–29% higher values of exergetic efficiency in the case of TFC system, depending on the inlet temperatures of heat source and cooling medium respectively. Nevertheless, the volume flow rate at the expander outlet was significantly higher in the TFC system, from 2.8 to 70 times greater than the ORC in the same operating conditions. Therefore, the author suggested the utilization of fluids with higher vapor pressures such as cyclopentane and butane. In a later study Lai and Fischer (2012), based on the same conditions described in Fischer (2011), carried out a comparison between TFC operating on organic fluids and water, an ORC and a Clausius-Rankine cycle. The TFC with water outperformed all the other cycles in terms of exergetic efficiency. To deal with the high flow rates at the expander outlet, the use of alkanes was advised. In Smith and da Silva (1994) the authors showed that the application of mixtures as working fluids can contribute to a better temperature match in the heat source and sink levels. This concept was confirmed in Zamfirescu and Dincer (2008) in which a comparison between TFC working with ammonia-water mixture, ORCs with four different organic fluids and a Kalina cycle was performed. In particular, TFC based on ammonia-water mixture outperformed all the other configurations in terms of exergetic efficiency and also it is capable of absorbing larger amount of heat available compared to the other technologies. Process modeling and optimization of TFC based on *n*-pentane, were conducted in the PhD thesis of Habeeb (2014). The author compared the performance of different TFC cycle architectures including reheating and regeneration. The maximum cycle temperature was 200 °C, while the condensing temperature and the expander inlet pressure were 36 °C and 30 bar respectively. The expander isentropic efficiency was set at 90%. The outcome of his study revealed that the TFC integrated with internal heat exchanger had greatest performance in terms of thermal efficiency, work output and exergetic efficiency.

Besides working fluid selection, the main constraint to the commercial development of TFC system is the two-phase expander. Some turbo-expander technologies (e.g. Euler turbine) are suitable in niche and large scale applications such as the cryogenic transportation of liquefied natural gas presented in Kimmel and Cathery (2010). However, in low grade heat to power conversion applications having a power output from tens to few hundreds of kilowatts, the issues related to a two-phase expansion tends to discard the turbomachines. Similarly, those positive displacement technologies that experience severe efficiency drops when high revolution speeds are required to match large flow rate demands should be also discouraged. For these reasons, the literature seems to identify twin-screw machines as the most suitable expansion technology for TFC. Nonetheless, some recent modeling studies on piston expanders by Steffen et al. (2013) showed promising values for isentropic efficiency (0.75–0.88 using water, 0.65–0.85 for ethanol and 0.50–0.70 with *n*-pentane) while experimental investigations by Kanno et al. (2015) showed that the deterioration of adiabatic efficiency with piston velocity could be reduced using a filter-type sintered metal fixed on the bottom of the cylinder to enhance boiling.

To date, few experimental activities on twin-screw expanders have been published. In particular, Kliem (2005) investigated the two-phase screw-type engine using water as the working fluid. He experimentally retrieved the isentropic efficiency of the expansion machine to be in the order of 30%−55%, depending on inlet temperature. Similarly, in Steidel et al. (1982) a 50 kW machine resulted in a peak adiabatic isentropic efficiency equal to 40% while in McKay (1982) a 1 MW helical screw expander showed a peak efficiency of 62%. On the other hand, the tests carried out in Smith et al. (1996) on a 45 kW machine using R113 revealed efficiencies up to 80%. In Öhman and Lundqvist (2013) a 42 kW machine was tested with R134a and resulted in a peak efficiency up to 92%.

Twin-screw machine modeling is a research topic widely investigated in the literature. A reference chamber model, that considers the spatial variation of quantities in the cavity built by male and female rotors lobes to be homogeneous, is presented in Stosic et al. (2005). On the other hand, three-dimensional com-

putational methodologies have been developed and tested with reference to air compressors in Rane and Kovacevic (2017), and for single phase ORC expanders in Papes et al. (2015). Two-phase twin-screw expanders have been mostly modeled with the lumped parameter approach which does not consider spatial variation of the fluid properties inside the control volume as well as in the leakage gaps. This assumption, however, is in contrast with the experimental results that are being carried out on two-phase flows. In particular, Triplett et al. (1999) and Kawahara et al. (2009) investigated two-phase flows in small passages that resemble leakage paths, while in Kanno and Shikazono (2016) experiments were carried out with reference to a piston expander. All the flow visualizations reported non uniformity of the two-phase flows and dependency on pressure, quality and velocity. With regards to previous TFC chamber models, in Vasuthevan and Brümmer (2016) and Qi and Yu (2016) reference working fluid was water while the model proposed in Smith et al. (1996) was further developed and exploited in Read et al. (2016) to outline optimized twin-screw expander configurations with reference to multiple working fluids. In this study, the authors eventually proposed a variable port design to tune the expander built-in volume ratio at off-design operating conditions. In all the afore mentioned modeling approaches, mass and energy equations proposed in single phase models were coupled with analytical expressions of the Virial equation of states or, alternatively, with subroutines linked to thermophysical property databases. Leakage flows were always modeled as equivalent orifices. In particular, theoretical leakage paths (i.e. discarding manufacturing tolerances and thermal effects) were derived either using geometrical models or directly from CAD geometries, as in Qi and Yu (2016).

Compared to the literature at the state of the art, the current research work aims at providing a general chamber modeling methodology to the academic and industrial communities. In order to do that, the modeling activity on the two-phase twin-screw expander has been developed in the commercial environment GT-SUITE^{TM}. Besides reproducibility, novel features of the study lie on the possibility to predict pressure pulsations during suction and discharge phases since intake and exhaust ducts were modeled with a one-dimensional approach. The proposed model is also suitable for transient analyses and can be integrated in the overall model of the TFC system such that control strategies can be tested. After introducing the modeling methodology, a sample test case representative of an industrial machine is presented and its pressure–volume and quality-angle diagrams are discussed. Parametric analyses at different operating conditions are eventually carried out to assess the thermodynamic and volumetric expander capabilities at off-design conditions.

2. Overview on the Trilateral Flash Cycle

Most of the exploitable low grade waste heat streams ($<100\,^{\circ}C$) are exhausts or effluents characterized by a linear temperature glide due to the absence of latent heat transfer phenomena. In conventional bottoming thermodynamic cycles for heat to power conversion like the ORC ones, the heat gain of the working fluid involves its phase change which in turn constraints the heat recovery process and leads to high exergy losses. In a Trilateral Flash Cycle, on the other hand, the heat recovery occurs without the vaporization of the working fluid and considers saturated liquid conditions at the inlet of the expansion machine. In this way, better temperature matching between heat source and working fluid is achieved even though, for the same thermal power recovery, the lack of phase change implies higher working fluid flow rates (i.e. greater pumping power) as well as larger heat transfer surfaces (i.e. higher investment costs for the heat transfer equipment).

Hence, in its essential architecture, a TFC system like the one in Fig. 1a is composed of two heat exchangers, a pump and an expander. Similarly to an ORC system, the working fluid is pressurized prior to the heat gain and cooled down after the expansion process in which the actual conversion of the fluid enthalpy to mechanical power takes place. Besides the lack of phase change during the heat recovery, the second major difference between TFC and ORC is the two-phase expansion of the working fluid, which involves large density changes. In this regard, Fig. 1 summarizes a parametric analysis carried out with reference to the working fluids and the methodology proposed in Bianchi et al. (2017). The goal of the theoretical study herein presented is to provide orders of magnitude and trends for the built-in volume ratio (BIVR) requirements of positive displacement machines dealing with TFC applications regardless of the expander technology.

Fig. 1b shows the built-in volume ratio requirements for a positive displacement expander operating between $70\,^{\circ}C$ and $20\,^{\circ}C$ for different inlet qualities. As confirmed by the logarithmic scale on the BIVR axis, most of the density change occurs between saturated liquid conditions and a quality around 0.10–0.15. This exponential trend is particularly steep for R245fa and R1233zd(E) while for propane and R1234yf is smoother. Therefore, operating at the theoretical inlet conditions of the TFC would require BIVRs up to 60 for most of the Hydro Fluoro Olefins considered while the maximum value for the selected hydrocarbons would be close to 20.

Within the acceptable operating temperature range of the working fluids and with reference to the saturation pressure which corresponds to a temperature of $20\,^{\circ}C$, Fig. 1c shows the built-in volume ratio that a positive displacement TFC expander with 70% isentropic efficiency and should have assuming that the expansion starts from a quality equal to 0.1. For all the working fluids considered, an increasing trend with the maximum cycle temperature can be clearly noticed due to the corresponding increase of the cycle pressure ratio. More importantly, all the working fluids show built-in volume ratio requirements below 10 for maximum temperature of the TFC not greater than $60\,^{\circ}C$. Lastly Fig. 1d displays the scarce influence of the expander adiabatic isentropic efficiency on the BIVR requirements for an inlet quality of 0.1 and at a temperature equal to $70\,^{\circ}C$.

A suitable TFC machine should be therefore be characterized by capabilities of handling large mass flow rates of two-phase fluids exposed to significant density changes especially in the first phases of the flash expansion. In this regard, in the so-called Smith cycle, Read et al. (2016) have considered the usage of multi-stage expansions and the combination of positive displacement machines and turbomachinery for the high and low pressure expansions respectively. On the other hand, with reference to less efficient but more cost effective single stage recovery system layouts, twin-screw expanders are currently one of the most promising machines thanks to intermediate values of built-in volume ratio achievable as well as the capability of rotating at high speeds without major performance drops.

3. Modeling approach

The commercial software environment in which the twin screw expander model has been developed is GT-SUITE^{TM}. Benefits of using this platform are the possibility of integrating sub-models of other TFC equipment (e.g. heat exchangers) to simulate full systems including controls. The commercial nature of the software further provides a standardization of the modeling procedure that is undoubtedly valuable at industrial level. From a research perspective, however, this fact constraints the implementation of customized models in the flow solver.

GT-SUITE^{TM} is based on a one-dimensional formulation of Navier–Stokes equations and on a staggered grid spatial discretization. According to this approach, each system is discretized into a series of capacities such that manifolds are represented by single volumes while pipes are divided into one or more volumes.

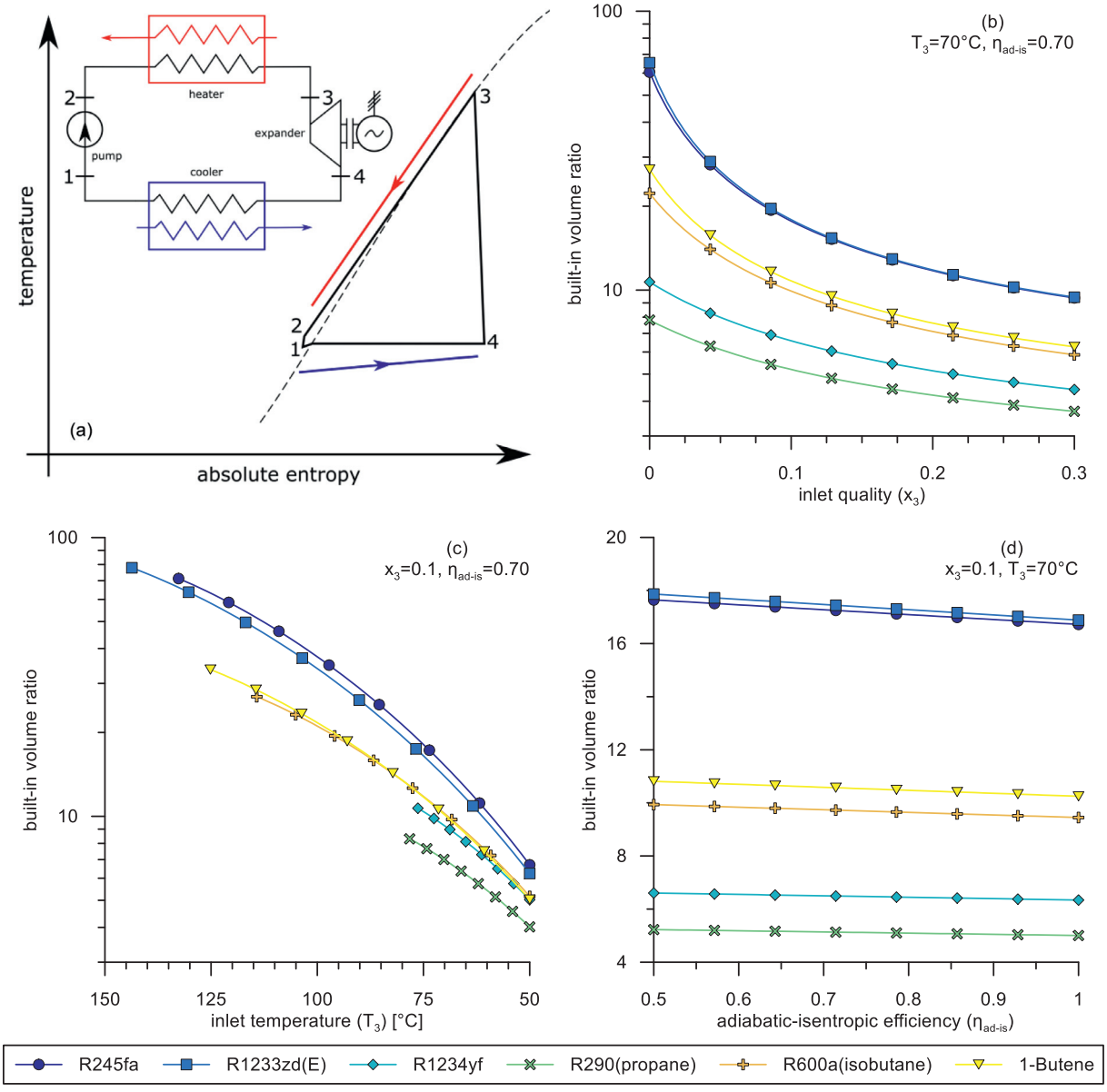

Fig. 1. Theoretical analysis of Trilateral Flash Cycle: scheme and entropy diagram (a), built-in volume ratio requirements for a positive displacement expander operating in a TFC system with condensation temperature (T_4) equal to 20 °C (b–d).

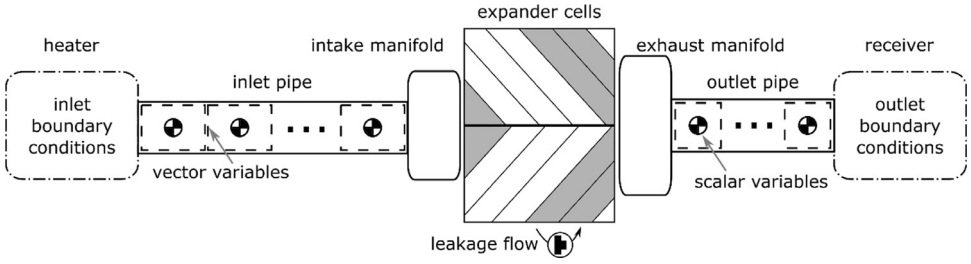

Fig. 2. Modeling scheme.

These volumes are eventually connected by boundaries. The scalar variables (pressure, temperature, density, internal energy, enthalpy, etc.) are assumed to be uniform in each volume. On the other hand, vector variables (mass flux, velocity, mass fraction fluxes, etc.) are calculated for each boundary (Gamma Technologies, 2017).

The schematic of the TFC expander model, which applies to any positive displacement machine, is reported in Fig. 2. Once discretized, in the inlet and outlet pipes the scalar equations (mass, energy) are solved at the centers of finite volumes, and the vector one (momentum) at the boundaries between them. The intake and exhaust manifolds are modeled as capacities of finite volume and connect the pipes with the filling and emptying expander cells respectively. These components are named “flowsplits” and have multiple openings whose number depends on the number of cells and of the leakage paths. The solution of the flowsplit is similar to the pipe: the scalars are solved at the center of the volume,

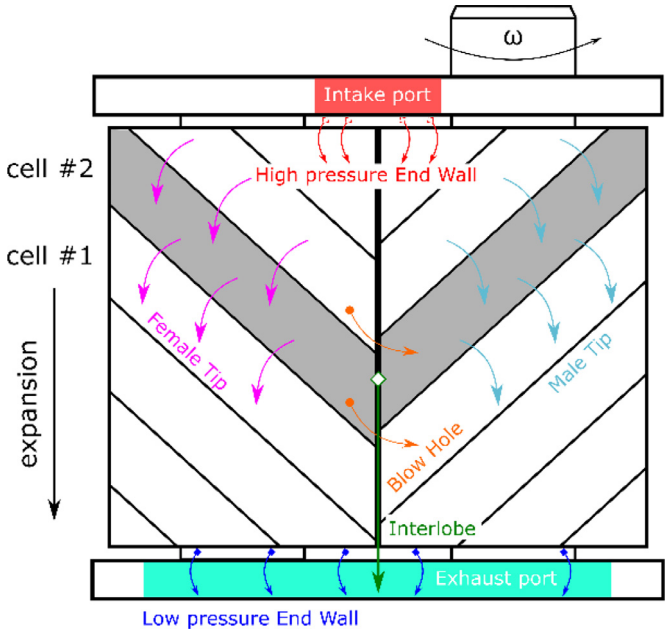

Fig. 3. Leakage paths in a twin-screw expander (elaboration from Fleming and Tang (1995)).

while the solution of the momentum equation is carried out separately at each of the volume openings (boundaries). The expander cells, that are physically generated when male and female rotor lobes engage, are treated as capacities with uniform properties and whose volume varies according to a law that is given as input of the calculation since the software does not provide a geometrical pre-processor yet. In addition to the revolution speed, inlet and outlet boundary conditions, which physically would be respectively provided by the heater and the receiver (or directly the condenser) of the TFC system, in this standalone model of the expander have been considered as plenums of infinite capacity.

As concerns the leakage paths, six different categories were identified according to the literature (Fleming and Tang, 1995) and reported in Fig. 3.

3.1. Governing equations

The continuity Eq. (1) in a given capacity takes into account the algebraic sum of all the inflow and outflow contributions from the neighboring capacities that occur through the B boundaries that characterize the reference element.

$$\frac{dm}{dt} = \sum_{i=1}^{B} \dot{m}_i \tag{1}$$

For instance, with reference to Fig. 2, the inlet manifold is characterized by one incoming flow from the inlet pipe at the left hand side boundary and $2Z$ outlet flows from the right hand side boundaries, out of which the half are the contributions that occur due to the Z expander cells during the suction phase while the remaining Z are due to the leakage flows through the high pressure end wall (Fig. 3). On the other hand, with reference to Fig. 3, the mass evolution in a given cell during the expansion depends on the values at the previous time steps, on the contributions due to the incoming and outgoing leakage flows with the adjacent cells as well as on the interlobe leakage.

The momentum Eq. (2) neglects body forces and takes into account the algebraic sum of momentums through the boundaries, pressure forces and dissipations due to friction and pressure drops. In pipes, the latter two terms are respectively related to distribute (i.e. due to surface finish) or concentrate (i.e. due to bends) pressure losses. In twin-screw expander cells, they have been herein discarded.

Table 1
Main geometrical and operating features of the expander.

Rotor diameter	127 mm
Aspect ratio (L/D)	1.65
Built-in volume ratio	5
Male/female rotor lobes	4/6
Suction/discharge ports arrangement	axial/axial
Revolution speed range	1500–6000 RPM
Tip speed range	10.01–40.06 m/s
Weight	220 kg

$$\frac{d\dot{m}}{dt} = \frac{1}{d\zeta}\left(\sum_{i=1}^{B}(\dot{m}_i u_i) + dpA - 4C_f\frac{\rho u|u|}{2}\frac{d\zeta A}{D} - K_p\left(\frac{1}{2}\rho u|u|\right)A\right) \tag{2}$$

The energy Eq. (3) states the conservation of total internal energy, i.e. the sum of internal energy and kinetic energy ($e = r + u^2/2$). Neglecting variations of potential energy, for a given capacity the rate of change of total internal energy depends on the volume capacity variations, on the enthalpy fluxes and on heat transfer phenomena. The first term on the right hand side of Eq. (3) relates to the cell volume, thus it is of paramount importance for positive displacement machines. Furthermore, since the model herein developed was assumed adiabatic with respect to the heat transfer from/to the casing and the rotors, the latter term in Eq. (3) has been discarded.

$$\frac{d(me)}{dt} = -p\frac{dV}{dt} + \sum_{i=1}^{B}\left(\dot{m}_i\left(e_i + \frac{p_i}{\rho_i}\right)\right) - HA_s(T_{\text{fluid}} - T_{\text{wall}}) \tag{3}$$

The conservation equations are solved through an explicit 5th order Runge–Kutta integration scheme whose primary solution variables are mass flow rate, density, and internal energy. In particular, to calculate mass and energy in a given volume at the following time step (that needs to satisfy the Courant condition for numerical stability), continuity and energy equations are firstly used and involve the reference volume and its neighbors. With the volume and mass known, the density is calculated and leads to density and energy. Using a dynamic-link library (DLL) of the NIST REFPROP database (Lemmon et al., 2010) embedded in the software package, the solver iterates on pressure and temperature until they satisfy the density and energy already calculated for this time step.

With regards to the calculation of quality during the expansion process, for the sake of simplicity, let us assume a changing volume with no leakage. In this case, the conservation of mass and momentum are trivial, which leaves only the term on the left hand side and the first term on the right hand side in the energy Eq. (3). With reference to an explicit solution scheme, the time step is firstly advanced to calculate the rate of change in the volume of the expander cell dV/dt. Knowing mass and pressure from the previous time step, the change in internal energy $dr = de$ can be therefore calculated. Finally, knowing density and internal energy, all the thermodynamic properties including the quality can be calculated by querying the REFPROP DLL.

3.2. Leakage flows

Similarly to any chamber modeling approach, leakages are herein considered as flow through an orifice. In particular, the incompressible Bernoulli equation is used for liquids while the isentropic nozzle relationships for subsonic (Eq. (4)) and chocked

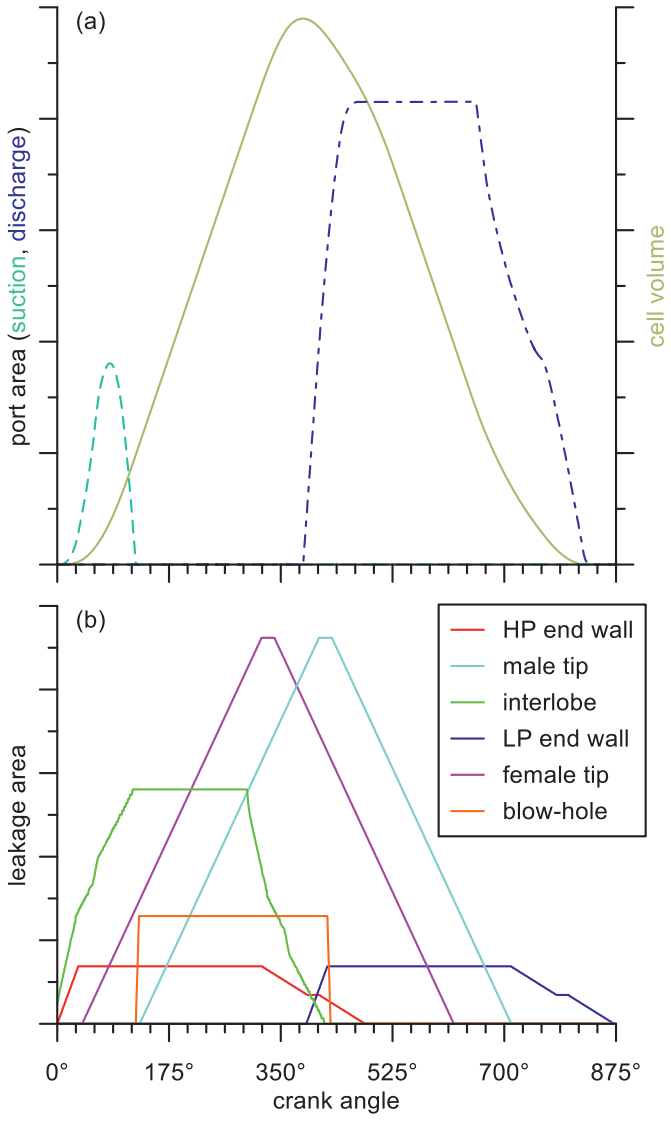

Fig. 4. Angular evolution of geometrical quantities: expander cell volume with suction and discharge ports (a) and leakage areas (b).

regimes (5) are considered for gases.

$$\dot{m}_{\text{leak}} = A_{\text{leak}}\left(\rho_{01}\left(\frac{p_2}{p_{01}}\right)^{1/\gamma}\right)\sqrt{RT_{01}\left(\frac{2\gamma}{\gamma-1}\left(1-\left(\frac{p_2}{p_{01}}\right)^{\frac{\gamma-1}{\gamma}}\right)\right)}^{1/2} \tag{4}$$

$$\dot{m}_{\text{leak}} = A_{\text{leak}}\left(\rho_{01}\left(\frac{2}{\gamma+1}\right)^{\frac{1}{\gamma-1}}\right)\sqrt{\gamma RT_{01}\left(\frac{2}{\gamma+1}\right)} \tag{5}$$

Two-phase leakage flows are calculated using the formulations valid for gases and assuming an equivalent ratio of specific heats γ as the weighted average, based on quality, of the ratio of specific heats for thermodynamic states at saturated conditions, as per Eq. (6). The same approach was used by Vasuthevan and Brümmer (2016) and Qi and Yu (2016).

$$\gamma = \gamma_{\text{vap}}x + \gamma_{\text{liq}}(1-x) \tag{6}$$

Conversely, Read et al. (2016) modeled the leakage through an orifice assuming as isenthalpic process whereas the leakage fluid is at the same thermodynamic conditions of the high pressure region. This approach involves the calculation of the dynamic viscosity of the two-phase fluid based on the quality and computed according to Eq. (7).

$$1/\mu = x/\mu_{\text{vap}} + (1-x)/\mu_{\text{liq}} \tag{7}$$

4. Simulation setup

The software GT-SUITE™ provides a template for chamber modeling but not a specific model for twin-screw machines yet. For this reason, the current approach does not consider any friction phenomenon and, in turn, won't be able to provide any insight on the mechanical efficiency of the machine.

4.1. Input data and boundary conditions

Fundamental inputs that have to be supplied to carry out the analysis are the angular evolution of geometric quantities such as cell volume, port areas and leakage paths. The calculation of these inputs is not trivial since it requires complex analytical models and, at the same time, plenty of information on the profile design. In the current case, the data on the TFC twin-screw expander,

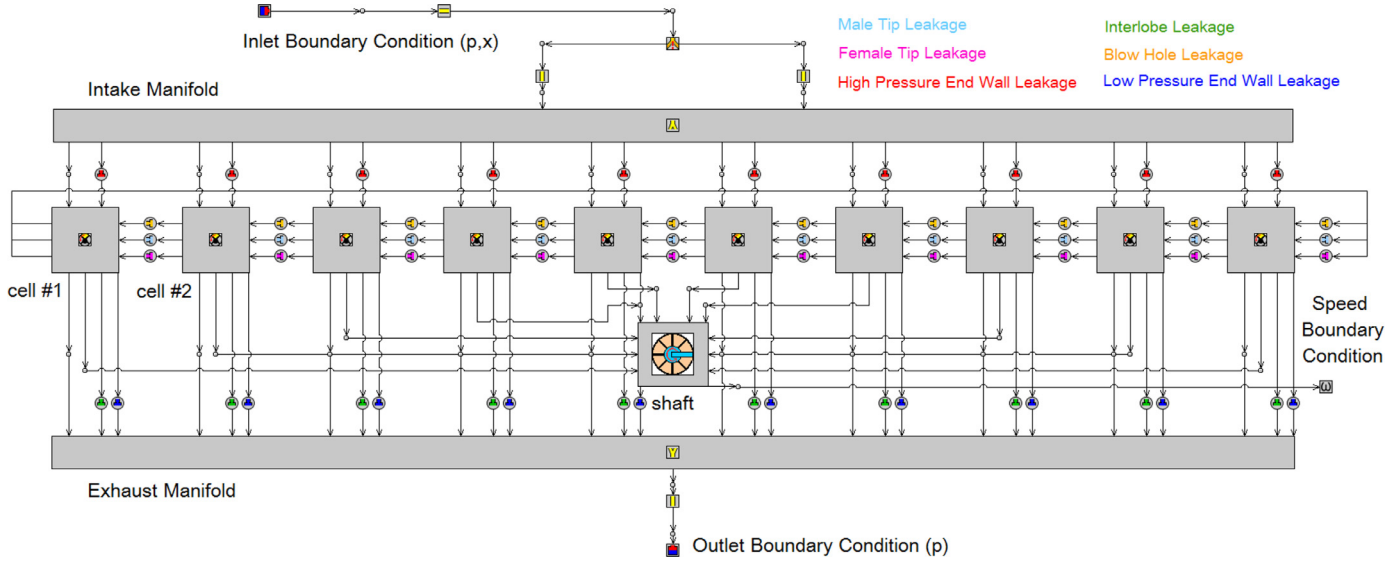

Fig. 5. Twin-screw expander model diagram in GT-SUITE™.

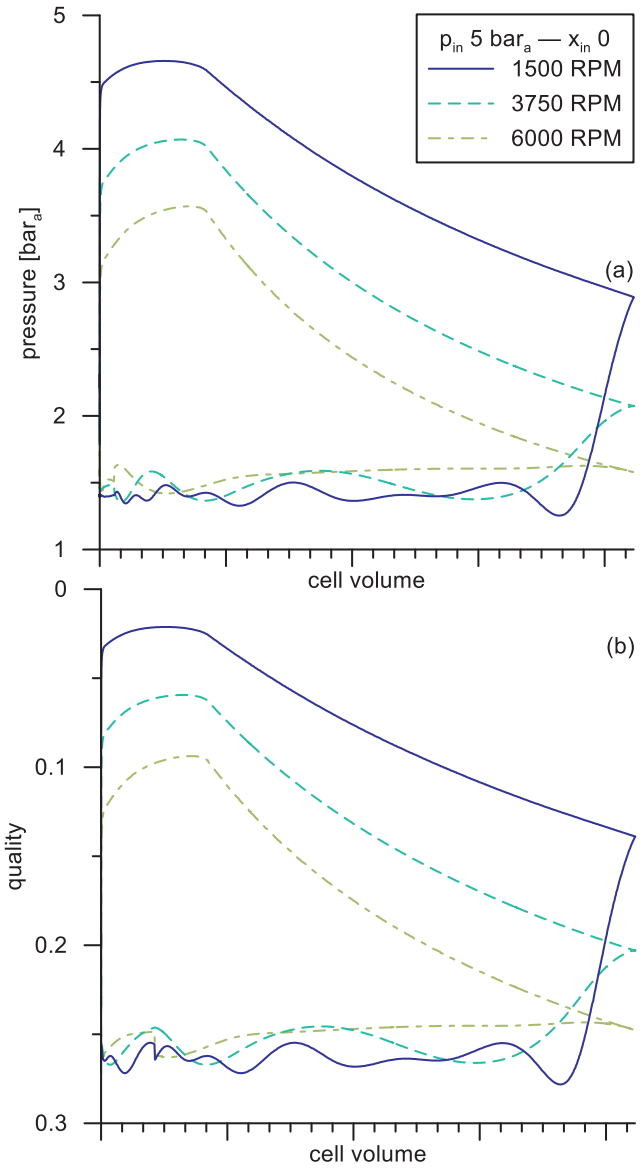

Fig. 6. Indicator (a) and quality (b) diagrams at low, medium and high revolution speeds.

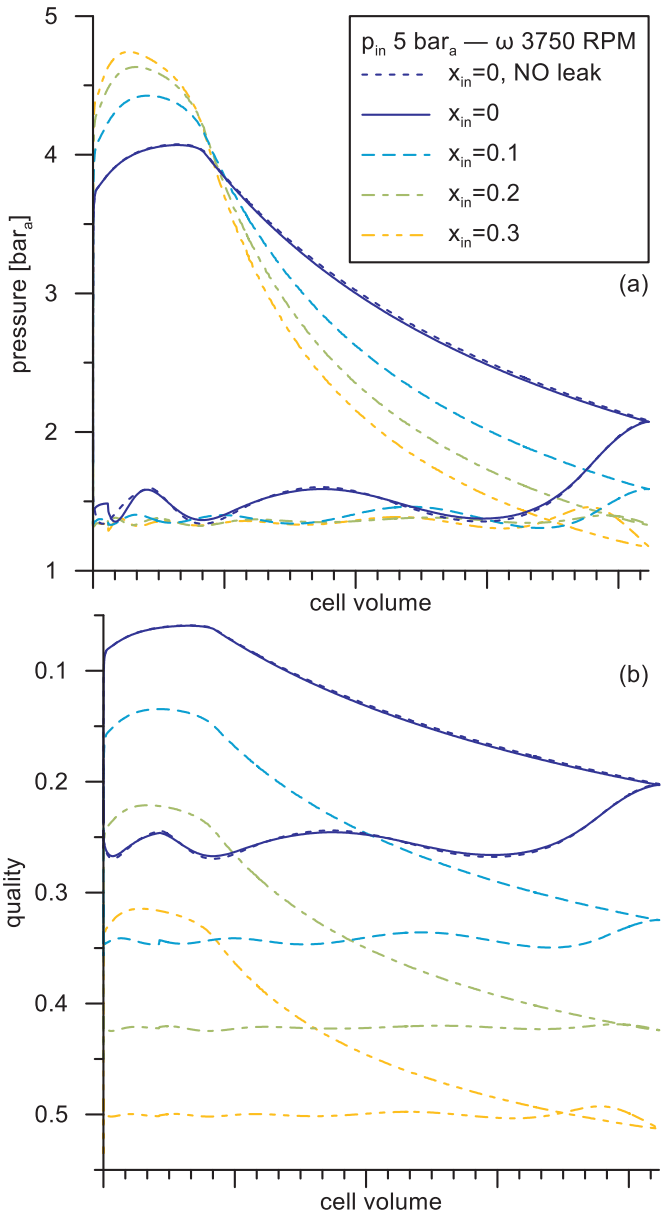

Fig. 7. Indicator (a) and quality (b) diagrams increasing inlet quality and in absence of leakages.

whose specifics are listed in Table 1, were provided by the manufacturer Howden Compressors Ltd.. Other valuable approaches are the development of customized geometrical pre-processors using literature correlations, retrieving geometrical quantities from CAD drawings as in Qi and Yu (2016) or using commercial software.

Fig. 4a shows the angular evolution of cell volume, suction and discharge areas while Fig. 4b reports the theoretical passage areas related to the leakage paths identified according to the literature (Fleming and Tang, 1995) and shown in Fig. 3. Equivalent orifices with the same colors represent the corresponding leakages paths in the model block diagram displayed in Fig. 5. These quantities are calculated based on geometrical quantities exclusively, without taking into account manufacturing tolerances. The effect of the operating temperature on the theoretical paths has also been neglected but the model could take it into account through empirical or semi-empirical correlations.

With reference to Fig. 5, the expander inlet is composed of two suction lines fed by the same boundary conditions (inlet pressure and quality) that a real TFC expander would see after the heat recovery process. The two feeding lines merge in the intake manifold through which the working fluid is made available to the expander cells during the suction phase. Similarly, after the closed-volume expansion phase, the contributions from the different cells merge in the exhaust manifold and eventually go through the outlet pipe toward the receiver or directly to the condenser. Hence, additional boundary conditions are the condenser pressure and the expander revolution speed.

In the reference machine, the angular cycle duration is 873°. In general, this quantity depends on geometrical quantities like the wrap angle. Due to the automotive nature of the software, GT-SUITE™ does not accept input quantities whose angular evolution is not a multiple of 360° (two-stroke engines) or 720° (four-stroke engines). Therefore, a scaling factor defined as in Eq. (8) was applied to shrink the angular cycle durations (but not the magnitudes) of the geometrical quantities in Fig. 4 to 360° as well as to the actual revolution speed ω_{real} to ensure that the mass flow rate calculated in a simulation cycle corresponded to the one which occurs during the actual operating cycle. With reference to the

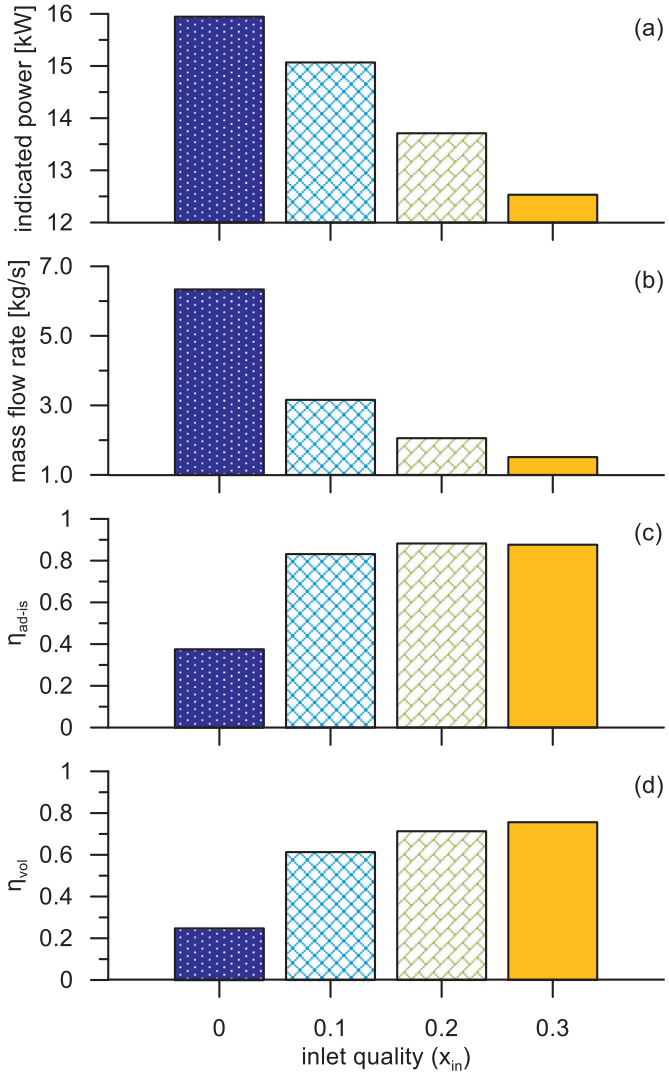

Fig. 8. Comparison of expander performance at increasing inlet quality.

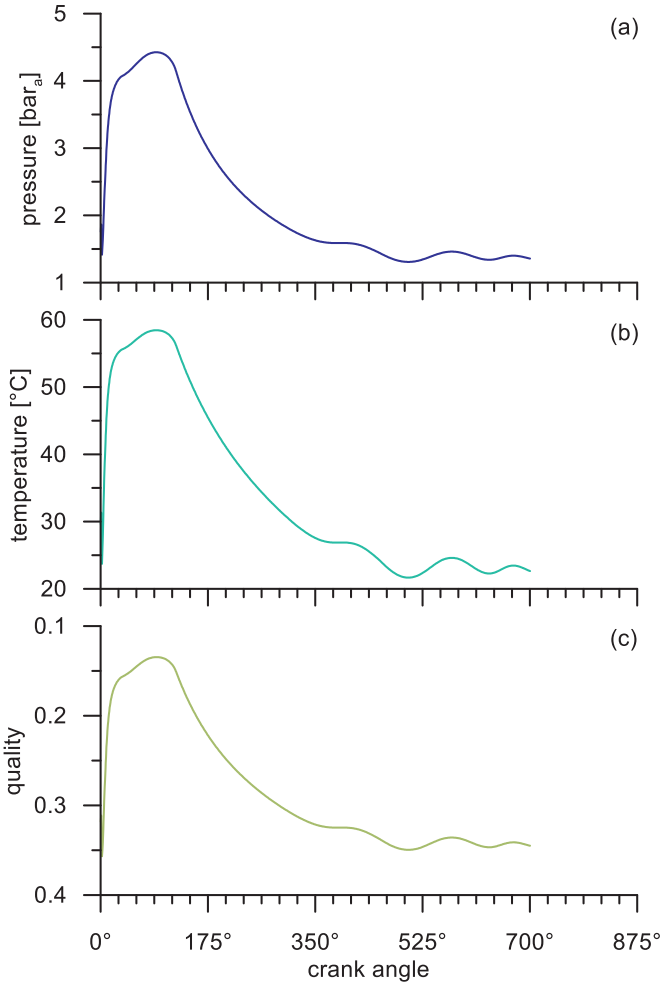

Fig. 9. Angular pressure (a), temperature (b) and quality (c) evolution at $x_{in} = 0.1$, 3750 RPM.

current study, the scaling factor was 0.412 (360°/873°).

$$SF = 360/\Delta\alpha = \omega_{sim}/\omega_{real} \tag{8}$$

Another tweak that was required to make the generic chamber model compliant to the expander investigated is the number of cells. In fact, from the number of lobes of the male rotor it results that the cell frequency is 4 times the one imposed by the revolution speed, i.e. each 90° of actual crank angle the expander has a cell that is discharging to the outlet manifold. At the same time, as shown in Fig. 4, a given cell takes 873° to reach twice the initial position α_0. During this interval, there will be nearly 10 cells (873°/90° = 9.7) that pass through α_0 (on an absolute frame of reference). Therefore, the number of cells to be modeled in GT-SUITE™ is the next integer number that results from the ratio of the angular cell duration and the number of lobes in the male rotor, as per Eq. (9).

$$Z_{sim} = \text{ceil}\left(\frac{\Delta\alpha\, Z_{male}}{360}\right) \tag{9}$$

Once the number of simulated cells is calculated and the input data of Fig. 4 are scaled for a 360° cycle duration, the geometrical input data between consecutive cells are shifted by an angular quantity equal to the cell passing frequency multiplied by the scaling factor (0.412•90° = 37.11° in the current case).

4.2. Output data

Among the results the model is able to provide, the most significant ones to characterize the performance of a positive displacement machines are mass flow rate, indicated power as well as volumetric and adiabatic-isentropic efficiencies. In particular, the equivalence of mass flow rate between simulations and actual operation of the expander is ensured through the procedure presented in paragraph 4.1. As concerns the indicated power, the definition implemented in the software is reported in Eq. (10). However, if one applies the definitions of scaling factor and number of simulated cells as per Eqs. (8) and (9), a systematic error due to the next integer approximation can be noticed. In this particular case, if the user considered the software result the indicated power would be overestimated of 3.1% (10/9.7).

$$P^*_{ind} = Z_{sim}\frac{\omega_{sim}}{60}\oint pdV = \text{ceil}\left(\frac{Z_{male}}{SF}\right)\frac{\omega_{real}\,SF}{60}\oint pdV \neq Z_{male}\frac{\omega_{real}}{60}\oint pdV \tag{10}$$

The same issue occurs in the definition of the volumetric efficiency, expressed as the ratio between calculated mass flow rate and the ideal one where the density is referred to the inlet duct,

as shown in Eq. (11).

$$\eta^{*}_{vol} = \frac{\dot{m}}{\rho_{suc} V_{suc} Z_{sim} \frac{\omega_{sim}}{60}} = \frac{\dot{m}}{\rho_{suc} V_{suc} \text{ceil}\left(\frac{Z_{male}}{SF}\right) \frac{\omega_{real}\, SF}{60}} \neq \frac{\dot{m}}{\rho_{suc} V_{suc} Z_{male} \frac{\omega_{real}}{60}} \tag{11}$$

To overcome these post-processing flaws that anyway do not corrupt the overall model correctness and robustness, customized performance relationships for indicated power and volumetric efficiencies were implemented using elementary calculation blocks that GT-SUITE™ provides, Eqs. (12) and (13) respectively.

$$P_{ind} = Z_{male} \frac{\omega_{real}}{60} \oint p dV \tag{12}$$

$$\eta_{vol} = \frac{\dot{m}}{\rho_{suc} V_{suc} Z_{male} \frac{\omega_{real}}{60}} \tag{13}$$

The adiabatic-isentropic efficiency is eventually calculated as the ratio of the real and the isentropic enthalpy drops across the expander, i.e. with inlet and outlet enthalpies measured at mid-length of the inlet and outlet ducts respectively, as per Eq. (14).

$$\eta_{ad-is} = \frac{h_{01} - h_2}{h_{01} - h_{2,is}} \tag{14}$$

5. Results and discussion

Prior to broader parametric analyses that yielded performance maps of the twin-screw expander, the impact of operating parameters such as revolution speed and inlet quality were assessed with reference to a TFC application having R245fa as working fluid and operating between 62.7 °C and 21.9 °C. At these temperatures, corresponding saturated absolute pressures are 5.00 bar and 1.32 bar respectively. The choice of the working fluid resulted from a screening procedure presented in McGinty et al. (2017), in which a theoretical model of the TFC system showed that R245fa (and its replacement R1233zd) is able to provide the largest net power output among a selection of working fluids for low grade heat to power conversion applications.

5.1. Indicator diagrams

Fig. 6 shows the effect of revolution speed on the expander indicator and quality diagrams. As mentioned in Section 3, the boundary conditions were inlet pressure and quality set at the inlet duct, outlet pressure set at the outlet duct and revolution speed. During the intake process, screw expanders tend to show pressure oscillations that however the model does not predict. This fact is likely due to the type of boundary conditions set at the inlet that, unlike the ones at the outlet, could not be set as an open boundary. Therefore, any backflow, which would have triggered pressure pulsations is suppressed.

At 1500 RPM, a 0.35 bar pressure decrease can be noticed during the suction phase since the volume of the intake manifold is larger than those of the inlet pipes to ensure a correct filling of the expander cells. However, this expansion does not produce any work. At the end of the suction phase, the closed volume expansion begins and brings the pressure down to 2.84 bar. As the expander cell opens toward the discharge port, the mismatching between the cell pressure and the outlet pressure of 1.32 bar triggers a sudden under-expansion. Without a detailed modeling, this passage would occur instantaneously, i.e. the mismatching between the built-in volume ratio and the manometric pressure ratio of the TFC expander would be compensated according to an isochoric transformation. In the current modeling approach, however, it can be noticed that this passage takes some crank angle degrees to develop. Furthermore, the sudden pressure change triggers some pressure oscillations during the discharge phase. For the same inlet and outlet conditions, the under-expansion noticed at 1500 RPM decreases at higher revolution speeds due to the enhanced expansion that takes place during the suction phase.

The effect of revolution speed on suction pressure similarly occurs for ORC expanders, i.e. when the working fluid is in superheated conditions during the suction process. However, in TFC machines, the transition toward states at increasing qualities is more enhanced. To reinforce this statement, Fig. 7 shows the indicator and quality diagrams at 3750 RPM for different inlet qualities. The difference with respect to the pressure at the inlet duct of 5 bar reduces as the quality of the incoming working fluid is increased. In particular, for saturated inlet conditions, the magnitude of the expansion at the inlet manifold during the suction phase is equal to 1 bar while for an inlet quality of 0.3 it reduces to 0.3 bar. The steeper pressure decrease for the simulations at greater inlet quality is due to the better volumetric efficiency of the machine as well as to the reduced magnitude of the flash expansion which, by releasing the latent heat of vaporization, contributes to perform an internal regeneration process. Fig. 7 additionally reports the comparison between indicator diagrams for saturated inlet conditions with and without leakages. Due to the marginal influence of the leakage on the pressure trend, we can conclude that the major player in the expander performance is quality.

The effect of inlet quality on the expander performance with respect to the simulations shown in Fig. 7 is reported in Fig. 8 in terms of mass flow rate, indicated power as well as volumetric and adiabatic-isentropic efficiencies. The high density at low quality allows to intake a greater amount of mass flow rate and contributes to achieve higher indicated powers, as shown respectively in Fig. 8a and b. However, the under-expansion during the closed volume phase and the increased expansion at the intake manifold lead to worse expander performance in terms of adiabatic-isentropic and volumetric efficiencies respectively, as reported in Fig. 8c and d. The best performing operating point is the one having an inlet quality equal to 0.1. Indeed, despite the slightly lower indicated power, this working condition allows to reach an adiabatic-isentropic equal to 83.1% and a volumetric efficiency equal to 61.2%. For saturated inlet conditions, these quantities would be equal to 61.3% and 24.8% respectively. On the other hand, greater inlet qualities would lead to better efficiencies but, at the same time, the indicated power would reduce from 15.1 kW at $x_{in} = 0.1$ to 13.7 kW and 12.5 kW at $x_{in} = 0.2$ and 0.3 respectively.

Fig. 9 shows the angular evolution of pressure, temperature and quality for the operating point at 3750 RPM and an inlet quality of the working fluid of 0.1. As the pressure drops from 4.40 bar to 1.32 bar, temperature decreases from 58.4 °C to 21.9 °C. On the other hand, quality increases from 0.14 to 0.35.

5.2. Performance maps

A broader operating range for the twin-screw expander was investigated through additional sets of simulations performed at different inlet conditions and revolution speeds from 1500 RPM to 6000 RPM. In particular, in Fig. 10 inlet pressure was varied from 5 to 10 bar at constant inlet quality equal to 0.125 while in Fig. 11 inlet quality was varied from saturated liquid to saturated vapor conditions at constant inlet absolute pressure equal to 7.5 bar. Outlet conditions were kept at 1.32 bar, as in Section 5.1.

Inlet pressure contributes on one hand to increase the density of the working fluid and, at the same time, leads to a higher manometric expansion ratio. For these reasons, in Fig. 10a and b greater

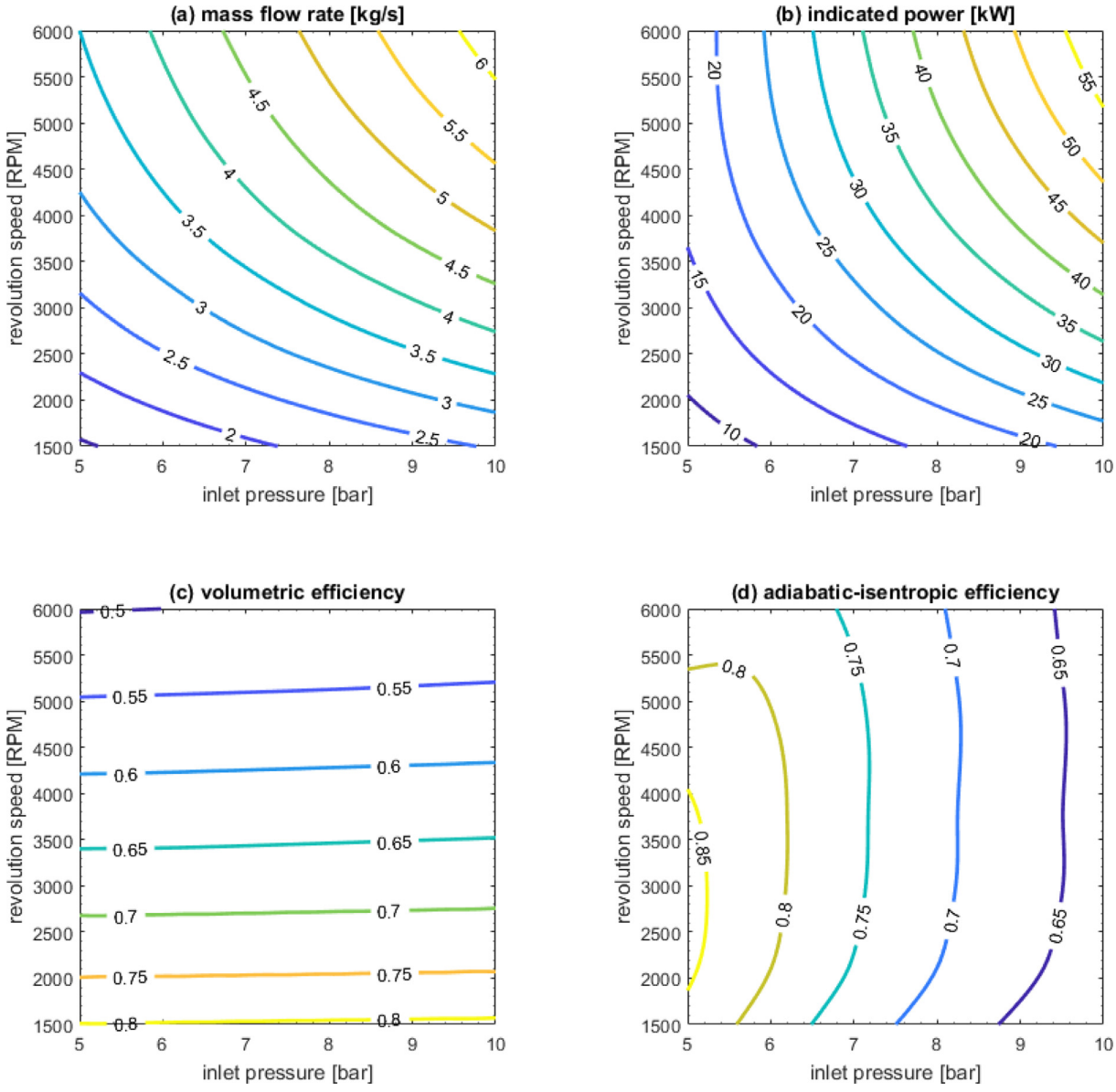

Fig. 10. Performance maps at different inlet pressures and revolution speeds ($x_{in} = 0.125$).

mass flow rates and indicated power can be respectively noticed. The effect on volumetric efficiency is slightly noticeable, although in Fig. 10c the slope of the iso-efficiency curves tends to increase at higher pressures. Because of the greater mismatching between built-in expansion ratio (equal to 5) and the cycle pressure ratio, the increasing magnitude of the under-expansion at higher inlet pressures leads the adiabatic-isentropic efficiency decrease, regardless of the revolution speed.

Due to the worsening of the volumetric efficiency, presented in Fig. 6 and additionally reported in Figs. 10c and 11c, the effect of revolution speed on mass flow rate and indicated power is still relevant. However, a given increase of revolution speed does not lead to the same percentage growth in performance. For instance, with reference to Fig. 10a and b, at 8 bar pressure inlet and 2500 RPM, mass flow rate is equal to 3.14 kg s^{-1} while indicated power is equal to 24.8 kW. If one doubles the revolution speed, mass flow rate is equal to 4.81 kg s^{-1} but not to 6.28 kg s^{-1} since volumetric efficiency drops from 73.7% at 2500 RPM to 57.5% at 5000 RPM. The same considerations apply for the indicated power that at 5000 RPM would be equal to 39.4 kW and not to 49.6 kW. On the other hand, with reference to Fig. 11d, beyond an inlet quality of 0.35, the effect of revolution speed on the adiabatic-isentropic efficiency are less noticeable due to the correct filling of the cell during the suction phase. As concerns the influence of the inlet quality, the lower density of the working fluid leads to lower mass flow rates (Fig. 11a) and, in turn, reduces the indicated power (Fig. 11b).

6. Conclusions

Low temperature heat to power conversion is an attractive opportunity for science and industry. However, the low exergy potential of the heat sources requires alternative thermodynamic cycle architectures to successfully recover and convert the waste heat potential. For this reason, the Trilateral Flash Cycle (TFC) might be a successful solution whose development still requires plenty of research efforts. In particular, the most challenging component in a TFC system is the expander since the efficient operation of this

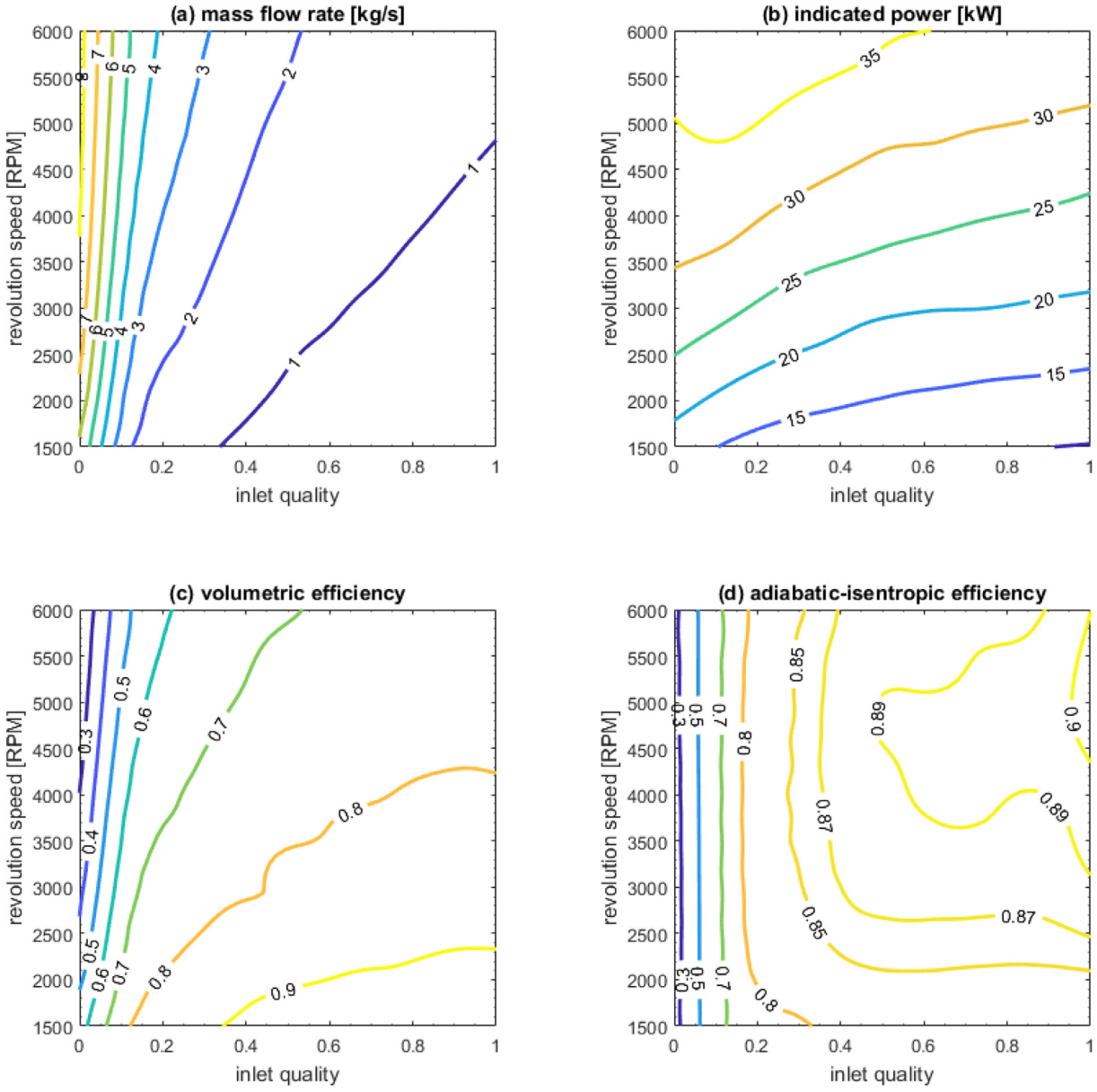

Fig. 11. Performance maps at different inlet qualities and revolution speeds ($p_{in} = 7.5$ bar).

machine directly impacts on the net power output. Due to the high mass flow rates and the intermediate pressure ratio that a TFC expander is required to operate with, among the positive displacement technologies, the twin-screw one seems to be the most suitable candidate. In order to fill the technological and knowledge gap in the field of two-phase expanders, the paper investigated a twin-screw TFC machine using a chamber modeling approach implemented in the commercial software GT-SUITE^{TM}. Benefit of using this platform is the integration potential with other sub-models of TFC equipment and with controls. After an extensive explanation of the modeling procedure to allow reproducibility of the results, the model of a twin-screw expander with 4/6 lobe configuration and a built-in volume ratio of 5 was developed and used to investigate the performance of the machine at different operating conditions. The most relevant outcome from the simulations was the impact of the expansion in the intake manifold on the overall machine performance. In fact, suction pressure at the expander cell may highly differ from the value at the inlet duct, especially if the machine is working at low inlet quality and high revolution speed. For a reference case at 3750 RPM and an inlet pressure of 5 bar, the best performing operating point resulted when the inlet quality of the R245fa working fluid was equal to 0.1. In these conditions, the expander volumetric efficiency was equal to 61.2% while the adiabatic-isentropic efficiency was 83.1%. On the other hand, if the expander operated with saturated inlet conditions, the afore mentioned performance parameters would be 24.8% and 37.6% respectively. The impact of the expansion in the inlet manifold on the overall machine performance could be improved by enlarging and shortening the manifold. The paper additionally presented indicator diagrams and performance maps of the twin-screw expander at a broad operating range. Despite the assumptions made on the calculation of the leakage flows and the lack of friction power modeling, the simulation platform can be successfully used to assess the performance of improved rotor profiles not only for TFC expanders but potentially for any twin-screw machine. Nevertheless, the validation against experimental data or more sophisticated numerical models is of paramount importance to further refine the current approach. Most of these activities will

be carried out based on data to be obtained from a full scale TFC system which will be tested in a real industrial application.

Acknowledgments

Research presented in this paper has received funding from: (i) the European Union's Horizon 2020 Research and Innovation Programme under grant agreement no. 680599, (ii) Innovate UK (project no. 61995-431253, (iii) Engineering and Physical Sciences Research Council UK (EPSRC), grant no. EP/P510294/1 and (iv) Research Councils UK (RCUK), grant no. EP/K011820/1. The authors would like to acknowledge the financial support from these organizations as well as contributions from industry partners: Spirax Sarco Engineering PLC, Howden Compressors Ltd, Tata Steel, Artic Circle Ltd, Cooper Tires Ltd, Industrial Power Units Ltd. The authors also acknowledge contributions from Mr. Jonathan Harrison and Mr. Marek Lehocky of Gamma Technologies during the model development. The manuscript reports all the relevant data to support the understanding of the results. More detailed information and data, if required, can be obtained by contacting the corresponding author of the paper.

References

Bianchi, G., McGinty, R., Oliver, D., Brightman, D., Zaher, O., Tassou, S.A., Miller, J., Jouhara, H., 2017. Development and analysis of a packaged Trilateral Flash Cycle system for low grade heat to power conversion applications. Therm. Sci. Eng. Prog. 4, 113–121. https://doi.org/10.1016/J.TSEP.2017.09.009.

Fischer, J., 2011. Comparison of trilateral cycles and organic Rankine cycles. Energy 36, 6208–6219. https://doi.org/10.1016/j.energy.2011.07.041.

Fleming, J.S., Tang, Y., 1995. The analysis of leakage in a twin screw compressor and its application to performance improvement. Proc. Inst. Mech. Eng. Part E J. Process. Mech. Eng. 209, 125–136. https://doi.org/10.1243/PIME_PROC_1995_209_239_02.

Forman, C., Muritala, I.K., Pardemann, R., Meyer, B., 2016. Estimating the global waste heat potential. Renew. Sustain. Energy Rev. 57, 1568–1579. https://doi.org/10.1016/j.rser.2015.12.192.

Gamma Technologies, 2017. GT-SUITE Flow Theory Manual.

Habeeb, A., 2014. A Study of Trilateral Flash Cycle For Low-Grade Waste Heat Recovery-To-Power Generation. Cranfield University.

Kanno, H., Hasegawa, Y., Hayase, I., Shikazono, N., 2015. Experimental study on adiabatic two-phase expansion in a cylinder for trilateral flash cycle. In: 3rd International Seminar on ORC Power Systems. Brussels.

Kanno, H., Shikazono, N., 2016. Experimental study on two-phase adiabatic expansion in a reciprocating expander with intake and exhaust processes. Int. J. Heat Mass Transf. 102, 1004–1011. https://doi.org/10.1016/J.IJHEATMASSTRANSFER.2016.06.081.

Kawahara, A., Sadatomi, M., Nei, K., Matsuo, H., 2009. Experimental study on bubble velocity, void fraction and pressure drop for gas–liquid two-phase flow in a circular microchannel. Int. J. Heat Fluid Flow 30, 831–841. https://doi.org/10.1016/J.IJHEATFLUIDFLOW.2009.02.017.

Kimmel, E., Cathery, S., 2010. Thermo-fluid dynamics and design of liquid-vapour two-phase LNG expanders. In: Gas Processors Association-Europe, Technical Meeting, Advances in Process Equipment. Paris.

Kliem, B., 2005. Fundamentals of the Two-Phase Screw-Type Engine. Universität Dortmund.

Lai, N.A., Fischer, J., 2012. Efficiencies of power flash cycles. Energy 44, 1017–1027. https://doi.org/10.1016/j.energy.2012.04.046.

Lemmon, E.W.W., Huber, M.L.L., McLinden, M.O.O., 2010. NIST standard reference database 23: reference fluid thermodynamic and transport properties (REFPROP). Version 9.0. Phys. Chem. Prop. https://doi.org/10.1234/12345678.

McGinty, R., Bianchi, G., Zaher, O., Woolass, S., Oilver, D., Williams, C., Miller, J., 2017. Techno-economic survey and design of a pilot test rig for a trilateral flash cycle system in a steel production plant. Energy Procedia 123, 281–288 doi:10.1016/j.egypro.2017.07.242.

McKay, R., 1982. Helical Screw Expander Evaluation Project Final Report DOE/ET/28329-1.

McKenna, R.C., Norman, J.B., 2010. Spatial modelling of industrial heat loads and recovery potentials in the UK. Energy Policy 38, 5878–5891. https://doi.org/10.1016/j.enpol.2010.05.042.

Öhman, H., 2012. Implementation and evaluation of a low temperature waste heat recovery power cycle using NH3 in an Organic Rankine Cycle. Energy 48, 227–232. https://doi.org/10.1016/j.energy.2012.02.074.

Öhman, H., Lundqvist, P., 2013. Experimental investigation of a Lysholm Turbine operating with superheated, saturated and 2-phase inlet conditions. Appl. Therm. Eng. 50, 1211–1218. https://doi.org/10.1016/j.applthermaleng.2012.08.035.

Papes, I., Degroote, J., Vierendeels, J., 2015. New insights in twin screw expander performance for small scale ORC systems from 3D CFD analysis. Appl. Therm. Eng. 91, 535–546. https://doi.org/10.1016/j.applthermaleng.2015.08.034.

Peris, B., Navarro-Esbrí, J., Molés, F., Mota-Babiloni, A., 2015. Experimental study of an ORC (organic Rankine cycle) for low grade waste heat recovery in a ceramic industry. Energy 85, 534–542. https://doi.org/10.1016/j.energy.2015.03.065.

Qi, Y., Yu, Y., 2016. Thermodynamic simulation on the performance of twin screw expander applied in geothermal power generation. Energies. https://doi.org/10.3390/en9090694.

Rane, S., Kovacevic, A., 2017. Algebraic generation of single domain computational grid for twin screw machines. Part I. Implementation. Adv. Eng. Softw. 107, 38–50. https://doi.org/10.1016/j.advengsoft.2017.02.003.

Read, M.G., Smith, I.K., Stosic, N., 2016. Optimisation of power generation cycles using saturated liquid expansion to maximise heat recovery. Proc. Inst. Mech. Eng. Part E J. Process. Mech. Eng. 231, 57–69. https://doi.org/10.1177/0954408916679202.

Smith, I.K., 1993. Development of the trilateral flash cycle system. part 1: fundamental considerations. Arch. Proc. Inst. Mech. Eng. Part A J. Power Energy 1990-1996 (vols 204-210). https://doi.org/10.1243/PIME_PROC_1993_207_032_02.

Smith, I.K., da Silva, R.P.M., 1994. Development of the trilateral flash cycle system Part 2: increasing power output with working fluid mixtures. Arch. Proc. Inst. Mech. Eng. Part A J. Power Energy 204–210. 1990–1996 https://doi.org/10.1243/PIME_PROC_1994_208_022_02 .

Smith, I.K., Stošič, N., Aldis, C.A., 1996. Development of the Trilateral Flash Cycle system: part 3: the design of high-efficiency two-phase screw expanders. Proc. Inst. Mech. Eng. Part A J. Power Energy. https://doi.org/10.1243/PIME_PROC_1996_210_010_02.

Steffen, M., Löffler, M., Schaber, K., 2013. Efficiency of a new Triangle Cycle with flash evaporation in a piston engine. Energy 57, 295–307. https://doi.org/10.1016/j.energy.2012.11.054.

Steidel, R.F., Weiss, H., Flower, J.E., 1982. Performance characteristics of the Lysholm Engine as tested for geothermal power applications in the Imperial Valley. J. Eng. Power 104, 231–240.

Stosic, N., Smith, I.K., Kovacevic, A. (Eds.), 2005, Calculation of Screw Compressor Performance, in: Screw Compressors: Mathematical Modelling and Performance Calculation. Springer Berlin Heidelberg, Berlin, Heidelberg, pp. 49–75.

Tchanche, B.F., Lambrinos, G., Frangoudakis, A., Papadakis, G., 2011. Low-grade heat conversion into power using organic Rankine cycles – a review of various applications. Renew. Sustain. Energy Rev. 15, 3963–3979. https://doi.org/10.1016/j.rser.2011.07.024.

Triplett, K.A., Ghiaasiaan, S.M., Abdel-Khalik, S.I., Sadowski, D.L., 1999. Gas–liquid two-phase flow in microchannels Part I: two-phase flow patterns. Int. J. Multiph. Flow 25, 377–394. https://doi.org/10.1016/S0301-9322(98)00054-8.

Vasuthevan, H., Brümmer, A., 2016. Thermodynamic modeling of screw expander in a Trilateral Flash Cycle. In: Int. Compress. Eng. Conf.

Walsh, C., Thornley, P., 2012. The environmental impact and economic feasibility of introducing an Organic Rankine Cycle to recover low grade heat during the production of metallurgical coke. J. Clean. Prod. 34, 29–37. https://doi.org/10.1016/j.jclepro.2011.12.024.

Wang, M., Wang, J., Zhao, Y., Zhao, P., Dai, Y., 2013. Thermodynamic analysis and optimization of a solar-driven regenerative organic Rankine cycle (ORC) based on flat-plate solar collectors. Appl. Therm. Eng. 50, 816–825. https://doi.org/10.1016/j.applthermaleng.2012.08.013.

Zamfirescu, C., Dincer, I., 2008. Thermodynamic analysis of a novel ammonia–water trilateral Rankine cycle. Thermochim. Acta 477, 7–15. https://doi.org/10.1016/j.tca.2008.08.002.